Design and application of a mobile-robot-based transducer system for cable fault detection

FINAL PROJECT REPORT

For course:

Projects in Computer Science and Engineering

30.05.2017

HALMSTAD UNIVERSITY

Mirjan Heubaum

Supervisor

Hassan Nemati

Table of Contents

List of Figures

List of Abbreviations and Symbols

Abbreviation	Meaning
ADC	Analog-to-Digital converter
AMR	Anisotropic magnetoresistive
e.g.	Example given (exampli gratia)
etc.	etcetera
GMR	Giant magnetoresistive
IC	Integrated circuit
i.e.	that is (id est)
LSB	Least Significant Bit
MFD	Magnetic flux density
SNR	Signal-to-Noise ratio

Symbol	Name of Symbol	Dimension
B	Magnetic flux density	T
E	Dielectric strength	V/m
F	Force	N
I	Current	A
R	Resistance	Ω
S	Sensitivity	V/T
V	Voltage	V

1 Introduction

This project is motivated by an issue concerning power supply through electricity grids. It is very difficult to handle defect underground power cables within a cheap and fast way. To improve this situation this project will combine knowledge of the areas power engineering, electromagnetic fields, embedded systems and robotics. The aim is to design a mobile-robot-based transducer system to detect weak spots in underground power cables.

1.1 PROBLEM DEFINITION

Most of the power transmission cables are made to lay overhead. However, the urbanization and influence by weather conditions lead to the increasing use of underground cables for power transmission. One of the advantage of using underground cables compared to overhead lines is that the weather conditions such as wind and thunder have less impact on the cables and it does not require space overhead. However, if a failure occurs in the underground cables, it is hard to locate the cable, its weak spot and to correct the defect. Nowadays there are some methods to handle these weak spots. The most common method is the time-domain reflectometer (TDR). The problem is that by using this method they can have an estimate of the position of the fault, but not the exact position. The rising demand for electrical energy increases the importance of uninterrupted power transmission and therefore it is important to find fast and cheap methods of locating faults.

1.2 BACKGROUND INFORMATION

The purpose of this project is to find a method to detect an underground cable and its weak spots from the surface of the earth. When an electric current is flowing inside the cable, there is an electromagnetic field around it. Therefore, finding cable faults by moving sensors above and along the cable to measure the intensity of its electromagnetic field seems like a cheap and efficient way to handle this issue. However, there are different types of underground cables. Usually cables are three-phased and carry three phase A.C. current. Furthermore, there are two common ways of formation called trefoil and flat formation [1], which should be considered. In this project the sensors should be mounted on a mobile robot, which is supposed to drive

overhead along an underground cable, analyse the data und hopefully, is able to find weak spots with the aim that an engineer can directly dig at that location. In addition, previous works will maybe be integrated to allow the robot to avoid obstacles. The robot consists of a changeable number of connected metal plates (one above the other), two wheels, two motors, a motor driver and batteries. It can get equipped with a Raspberry Pi and different sensors like an infrared sensor. By mean of infrared sensors, the robot could be able to avoid obstacles. However, the main part of this project will be the investigation on the efficiency of electromagnetic sensors.

1.3 RELATED WORKS

There are related works which deal with detecting cables. In one experimental study called "Magnetic Field Measurement to Detect and Locate Underground Power Cable" a search coil was used successfully to measure the magnetic field of an underground cable and to define its position i.e. the depth and the coordinates relatively to the measurement points [2]. A right dimensioned search coil is a relatively good choice for detecting alternating fields, but its size is not comparable with the size of other types of sensors and therefore, difficult to integrate in a small robotic system. Then there are some works using other types of electromagnetic sensing, but they don't deal with cable faults [2] [4]. Moreover, some studies used electromagnetic sensing to detect cable faults, but they either let the sensor work directly on the cable, not on the ground surface or they used signal generators, which transmitted signals with higher frequencies than the 50 Hz through the cable [5] [6]. This work differs, because it has the aim to have a robot driving above the cable on the ground surface which can detect the magnetic field of an underground power cable and beyond that to detect a weak spot. However, it can make use of the experiences made in the related works.

Moreover, this work is based on a previous work of Ryota Iida at Halmstad University. It involved the use of a Hall effect sensor with the Raspberry Pi but did not succeeded in detecting cables.

2 Theory

## 2.1 THEORY OF ALTERNATING MAGNETIC FIELDS

Magnetic fields are based on the magnetic effect of electric currents or magnetic materials. The magnetic field has a direction and a magnitude and is therefore a vector field. The magnetic flux density (MFD) B is defined in terms of force on moving charge in the Lorentz force law:

$$\vec{F} = q\vec{E} + q\vec{v} \times \vec{B}$$

The SI unit for magnetic flux density is the Tesla, which can be deduced from the magnetic part of the Lorentz force law:

$$F_{magnetic} = qvB \leftrightarrow B = \frac{F}{qv}$$

$$[\vec{B}] = \frac{N * s}{C * m} = T \quad 1T = 10,000 \; Gauss$$

Figure 1: B-Field around wire
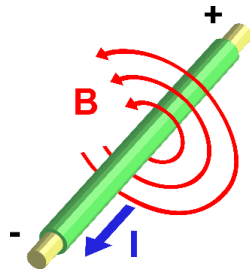
The magnetic field lines around a long wire, which carries an electric current, form concentric circles around the wire. The direction of the magnetic field is perpendicular to the wire. The magnetic field generated by a steady current I, μ_0 is the magnetic constant, is described by the Biot–Savart law:

$$|\vec{B}| = \frac{\mu_0 I}{4\pi * r} \int_{wire} \frac{dl * \hat{r}}{r^2}$$

The magnetic flux density of a current flow I through a very long conductor measured at the distance r:

$$|\vec{B}| = \frac{\mu_0 * I}{2 * \pi * r} \quad [B] = T$$

Therefore, the magnetic flux density is proportional to the current I. If there is an alternating current through the wire, the B-field will alter the same way. Because of its characteristics as a vector field, it can be cancelled with a field of the same magnitude in the opposite direction.

This can happen when for example one conductor is carrying the same current in the opposite direction of the other conductor and these conductors are close together.
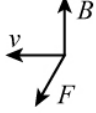
2.2 SENSORS

The most important aim is to find a suitable sensor for this purpose. Many different types of technologies are used to detect magnetic fields respectively the magnetic flux density. A very famous one is the Hall-sensor, which can measure constant fields but is not very accurate. Then there are different types of magneto-resistive sensors, which change their resistance when a magnetic field is applied. The most accurate is called SQUID, based on superconductors. To mention one more famous magnetic sensor there is the coil based magnetic sensor, known from the "search coil" [2].

2.2.1 Hall effect sensors

The Hall effect takes place in a thin flat conductor which carries electrical current when placed in a magnetic field. Due to the resulting Lorentz force, the moving charge carriers tend to flow on one side of the conductor. Therefore, on one side, there is a surplus of electrons and on the other side a lack of electrons. A measurable voltage between both sides is generated. The voltage is perpendicular to the magnetic field and to the current flow and proportional to the magnetic flux density B. It is called Hall voltage, V_H.
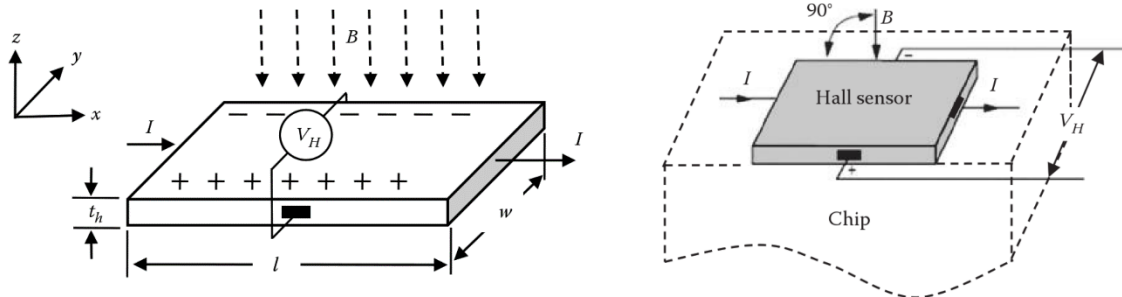
$$V_H = R_H * \frac{I * B}{d}$$

Figure 2: Hall element [7]

The operating principle of Hall sensors is based on the above-mentioned effect. One feature is the possibility of bringing the Hall sensor and signal processing units e.g. amplifier on one silicon ship, what allows low-cost production. Another advantage is a wide measurement range, but it has a low measuring accuracy.

A Hall device is typically packaged in a 3-pin single in-line package (SIP) for through-hole mounting. However, it is also available in smaller surface-mount packages e.g. micro leadframe package (MLP). [8]
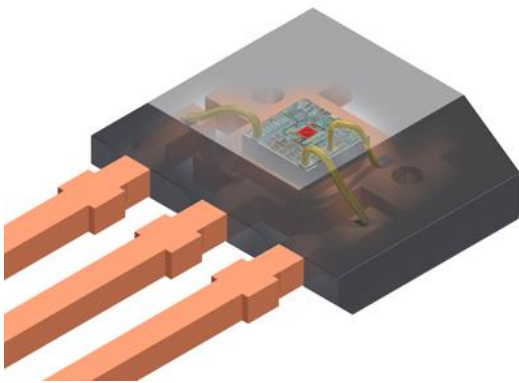
Figure 3: Hall device packaging example (SIP) [8]

2.2.2 Magnetoresistive sensors

Magnetoresistance is the effect of a material to change the value of its electrical resistance when a magnetic field is present. There is a small decrease in resistance in the transverse direction of an applied magnetic field and a small increase in resistance in the direction of the field. The intensity of this effect depends on the material of the conductor and can be described with the unitless value

$$M_R = \frac{\rho_B - \rho_0}{\rho_0} * 100\%$$

The MR effect can be class-divided in six different classes: OMR, AMR, GMR, TMR, BMR and CMR where the AMR (anisotropic magnetoresistance) and GMR (giant magnetoresistance) are significant in common magnetic sensing applications.

AMR

The use of ferromagnetic materials in magnetic fields leads to the AMR effect. The resistance of the material depends on the relationship of the current direction and the magnetic field direction. When they are parallel, the resistance reaches its maximum and otherwise, when they are perpendicular, it reaches its minimum. Typically, the AMR effect has a magnitude of around $M_R = 1\%$.

GMR

When using alternating ferromagnetic and metallic layer structures the GMR effect takes place. A simple three-layer structure e.g. FM-Metal-FM can be used to display the GMR effect, which can reach a magnitude of $M_R > 200\%$.

There are two different circuits to read the AMR/GMR sensors resistance. The simpler one is the series circuit with two elements also called voltage divider. By supplying two perpendicular arranged AMR/GMR sensors with a supply voltage, the voltage between the sensors and ground will change with the magnetic field. A more sensitive way is to use a Wheatstone bridge which consists of four elements. In that case, AMR1 and AMR3 have to be arranged perpendicular to AMR2 and AMR4. [7]
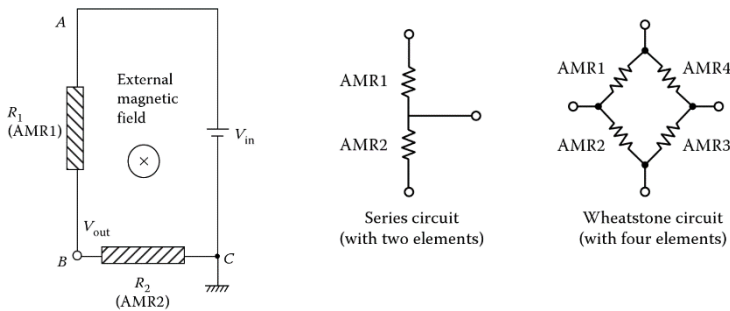
Figure 4: AMR sensor sognal conditioning (1. set-up of series circuit, 2. series circuit, 3. Wheatstone circuit [7]

2.2.3 SQUIDs

SQUIDs (superconducting quantum interference devices) are the most sensitive magnetic sensors available today. It is possible to detect magnetic field variations lower than 1 fT (i.e. 10^{-15}T). The working principle is based on superconducting loops interrupted by Josephson junctions. A constant current is carried through a ring with non-conductive films (Josephson junctions). Without magenetic field, the input current is splitted equally caused by the current

divider. When an external magnetic field is applied to the loop, there appears a current, which circulates. The effect is measurable by mean of the voltage. [9]
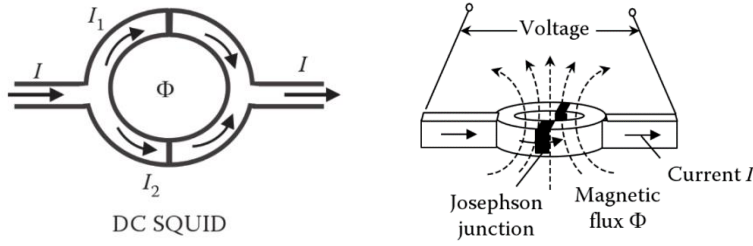
Figure 5: SQUID working principle [7]

As an example, SQUIDs are used in medical diagnostics to monitor the brain activities. The disadvantage is its need of an extremely low temperature provided by liquid nitrogen and a very small measuring range.
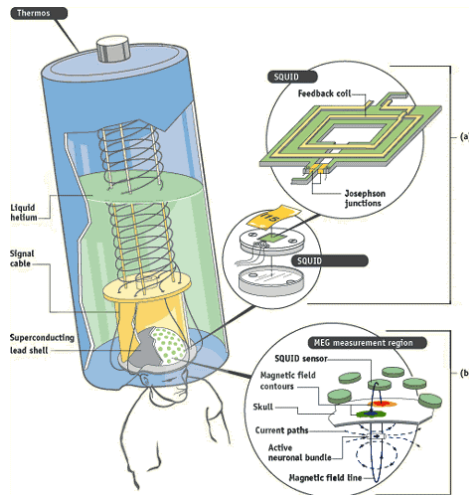
Figure 6: Brain activity measurement [8]

2.2.4 Coil based sensors

The coil based sensor (search coil) uses the Faraday's law of induction and is one of the simplest magnetic field sensing devices. It consists of N loops of wire. The voltage e will be induced by a temporal variation of the magnetic flux Φ through a N turns circuit. The voltage is proportional to the rate of change of the magnetic flux.

$$e(t) = -N\frac{d\Phi}{dt}$$

If a uniform field B is applied to the loop, the magnetic flux passing through the area A enclosed by the loop is

$$\Phi = B * A$$

The voltage becomes

$$e(t) = -N \frac{d(B * A)}{dt}$$

An advantage regarding this application is the fact that the coil based sensor will only measure the alternating part of the magnetic field, that would be a positive feature for this application. However, the coil is too big for an implementation on a robot. [8]

Figure 7: Copper Coil [8]

2.3 POWER CABLES

Sweden's power cable infrastructure is divided into a high-voltage transmission net with a voltage range of 40-130 kV, and a regional net with a voltage range of 10-20 kV. Underground cables are installed at depths of minimum 0.45 m depending on their voltage. There are two formations of three-phase underground power cables, called trefoil formation and flat formation. Depending on the formations the magnetic flux density differs. [3]

2.3.1 Partial Discharge

In electrical engineering, the phenomenon of partial discharge is a dielectric breakdown between two conducting electrodes across a localised area of the insulation. It can occur in high voltage systems at voltages above 3 kV in a gaseous, liquid or solid insulating medium. Voids in the medium and high electrical stress above a critical strength lead to this phenomenon. Air has a dielectric strength of 3 kV/mm whereas Polyethylene has a higher strength of 20-160 kV/mm. When there is a void in the insulator filled with air and the electric stress exceeds the electrical breakdown strength of the gas, the partial discharge begins within this gas void. Electrons move through the gas towards the more positive conductor and collide with the insulator causing aging of it. The moving electrons create an electric current (I=dq/dt). [12]

3   Experiment on the sensor system

The first methods were simulations of power supply cables and an experiment for measuring the magnetic field caused by such a cable.

3.1   SIMULATION

To get some information about what kind of magnetic fields can be expected a simulation tool called COMSOL Multiphysics was used.

3.1.1 Single-phase electric power

Due to the easier way of building an experimental setup with single-phase electric power systems compared to three-phase systems, it was helpful to simulate these systems first. In the simulation, there are two conductors of copper arranged side by side. In a common power supply cable for an electric device both conductors are very close and that is why the magnetic field will be cancelled.

If the distance between the conductors was increased, the magnetic flux density measured above the arrangements centre increased, too. If the distance was close to zero, the magnetic field was almost cancelled. Figure 8 shows the magnetic flux density of the abovementioned arrangement. The arrows emphasize the magnitude and direction of the B-field. The graph in figure 9 is based on the measurement in the simulation during the increase of the distance between the conductors and emphasizes the relation between inter-conductor distance and strength of the magnetic field.
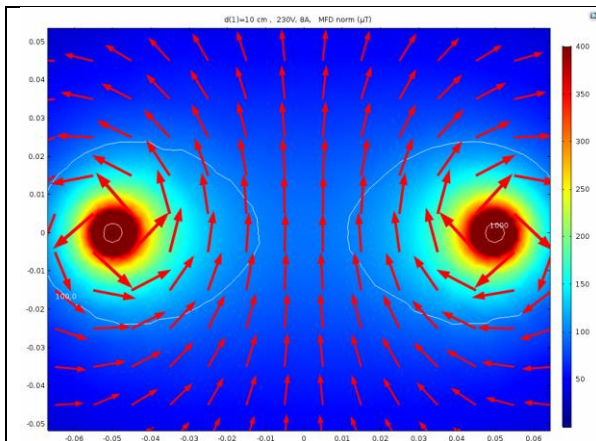
Figure 8: B-Field in one-phase system
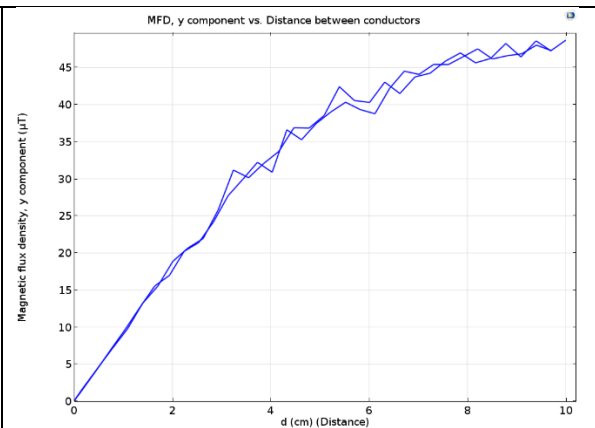
Figure 9: MFD vs. distance between conductors

The figures 10 and 11 show the MFD norm in comparison to the MFD y component.

Figure 10: MFD norm in one-phase A.C. system
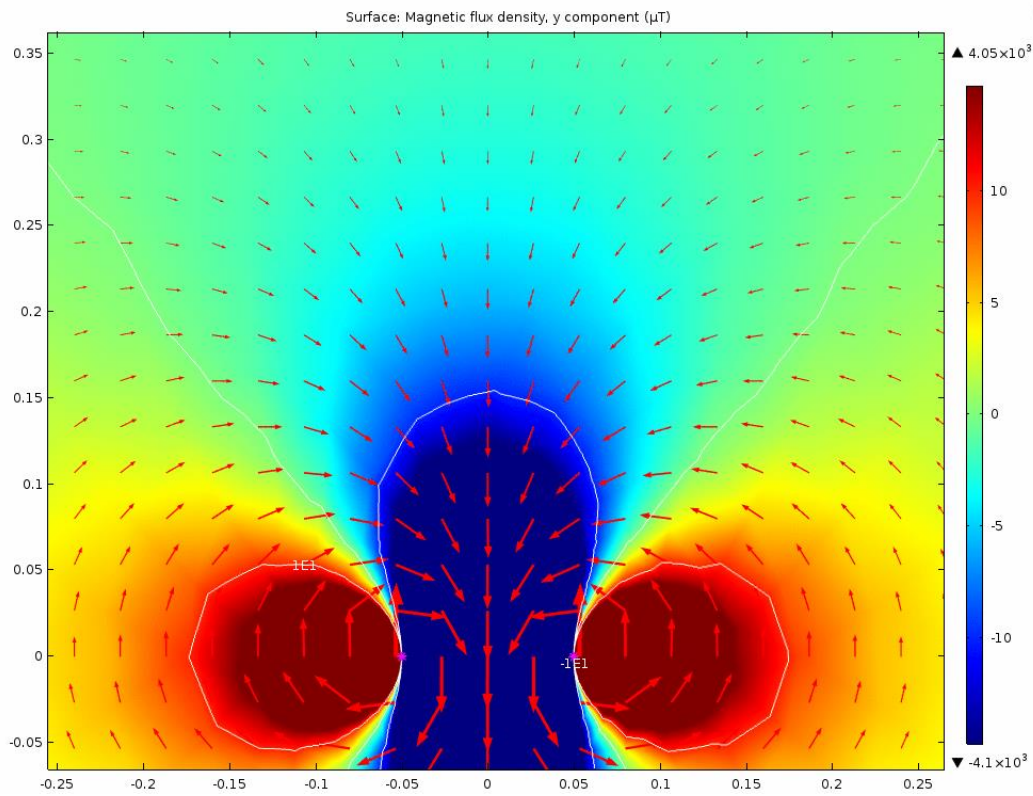
Figure 11: MFD y-component in one A.C. system

The table shows the sinusoidal wave of the alternating y-component of the magnetic flux density at different distances (1cm, 7cm, 14cm).
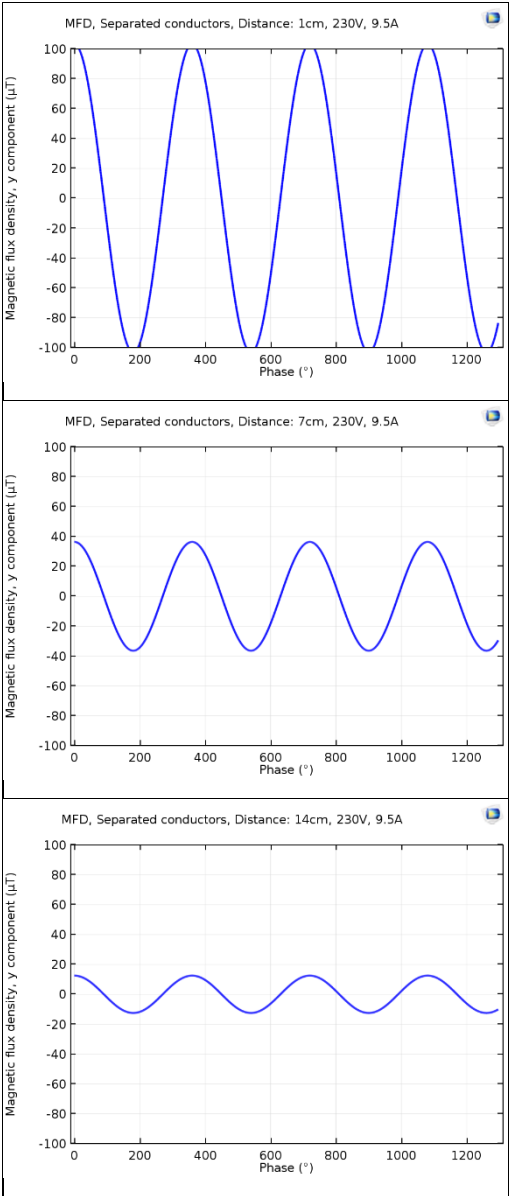
Figure 12: Sinusoidal wave of y-component of MFD in one-phase A.C. system

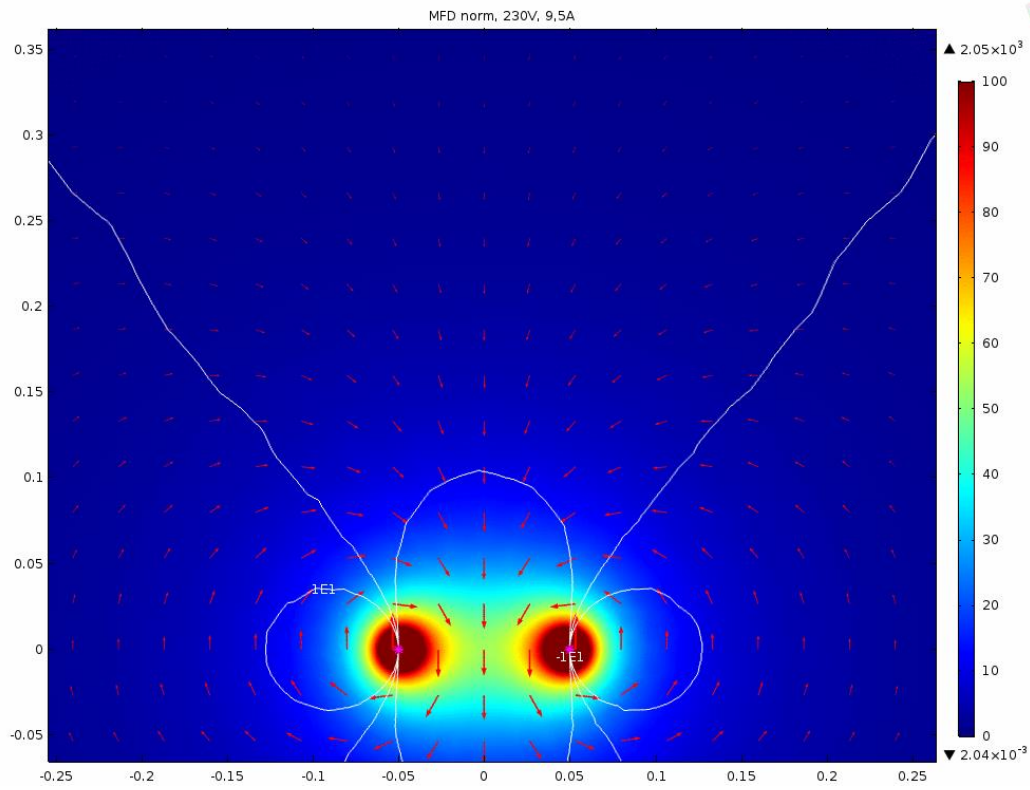## 3.1.2 Three-phase electric power

When it comes to underground power cables with three conductors, there are two different formations. The flat formation with the three conductors arranged side by side and the trefoil formation with a triangular arrangement of the conductors. Now a higher measuring distance should be used, because of the cables depth below ground. However, there are also much higher currents compared to low voltage applications.

Flat Formation	Trefoil Formation
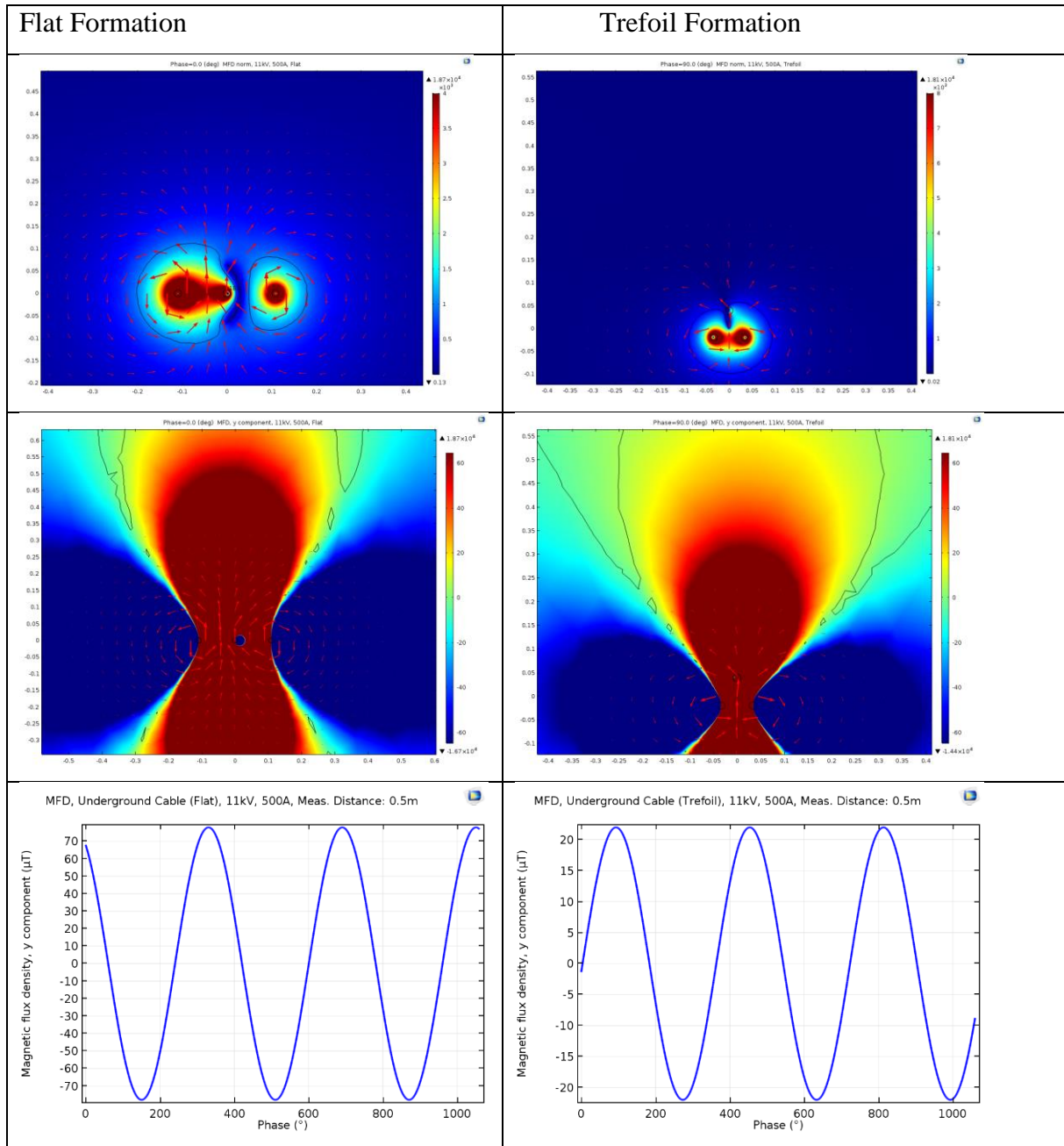
Figure 13: Simulation of MFD in three-phase A.C. system

The table shows that the magnetic flux density of the flat formation is much higher than the magnetic flux density of the trefoil formation, but both should be measurable according to the amplitude.
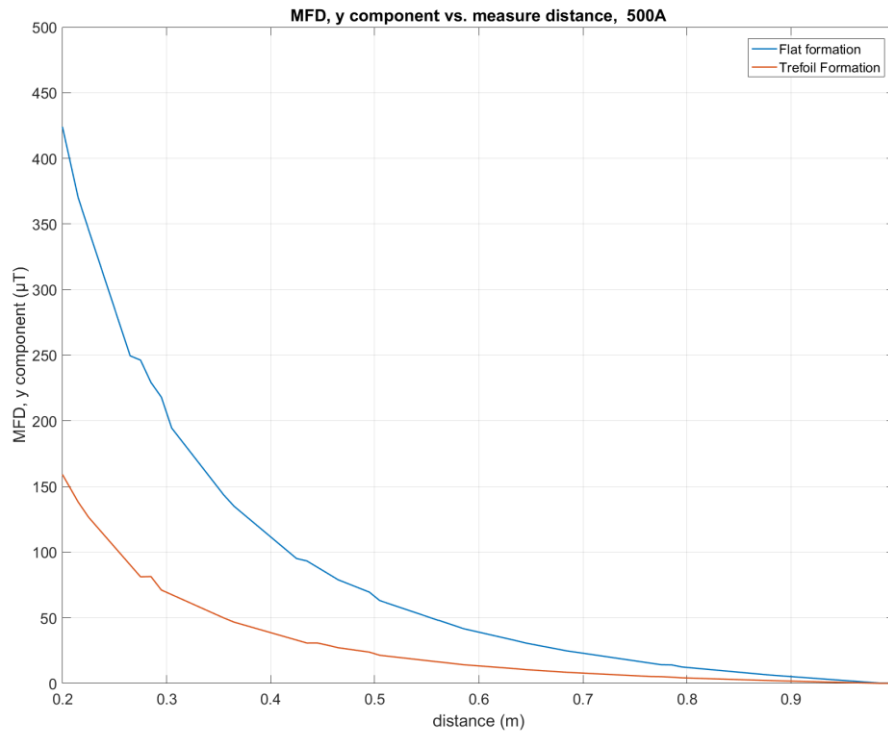
Figure 14: Simulated MFD in three-phase system vs. measuring distance

Figure 14 shows the magnetic flux density against the measuring distance. The relation is important because underground power cables are buried in different depth.

3.2 EXPERIMENT

After an unsuccessful first try with a common single-phase power supply cable for a water boiler, it was necessary to build an experimental setup. The theory of magnetic fields showed that the magnetic field is almost cancelled if the centres of both conductors in a single-phase system are to close. Therefore, a plank was the basis for a cable and two wall sockets. The three objects are typically used for electrical installation. The cable had three conductors and was connected to a socket on each end. In the middle part of the cable the insulation was removed and the two current carrying conductors were separated with approx. 10cm distance, like in the previous simulation. One socket was connected to the electricity grid and the other was connected to a big electrical load, which caused a current of approximately 9.5A. With one sensor placed above the centre of the plank with different heights (1cm, 7cm, 14cm) the measurements were started. Figure 15 shows the experimental setup.
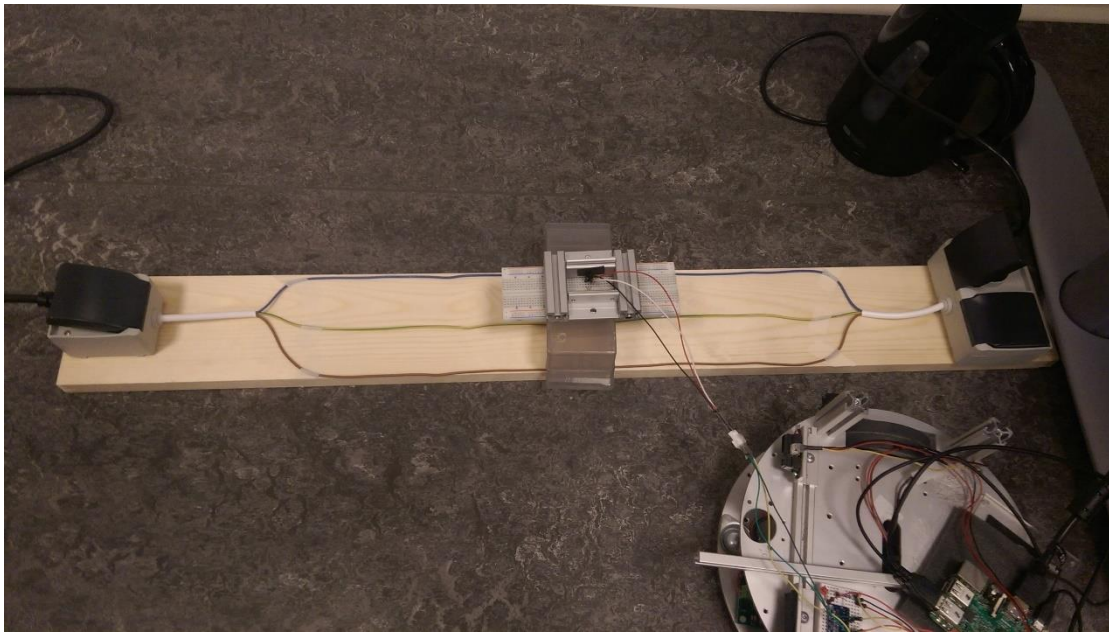
Figure 15: Experimental setup for verification of simuation

Within each measurement series with different distances between the sensor and the plank resp. the centre of the two conductors, the detection of an alternating magnetic field was possible. As expected, the measured data fits to the simulation of the y component of the magnetic flux density at each height. Figure 16 shows a comparison of the simulated magnetic flux density (left) and the measured flux density (right). In a measuring distance of 1cm the magnetic flux density amplitude amounted approx. 100µT, 7cm above the plank it was 40µT and 14cm above less than 20µT.

Figure 16: Comparison of simulation and experimental results

4 Mobile robot as sensor carrier

The mobile-robot-based transducer system consists of a changeable number of connected metal plates (one above the other), two wheels, two motors, a motor driver and batteries. The robot is equipped with a Raspberry Pi 3 for data processing. The first chosen sensor is a 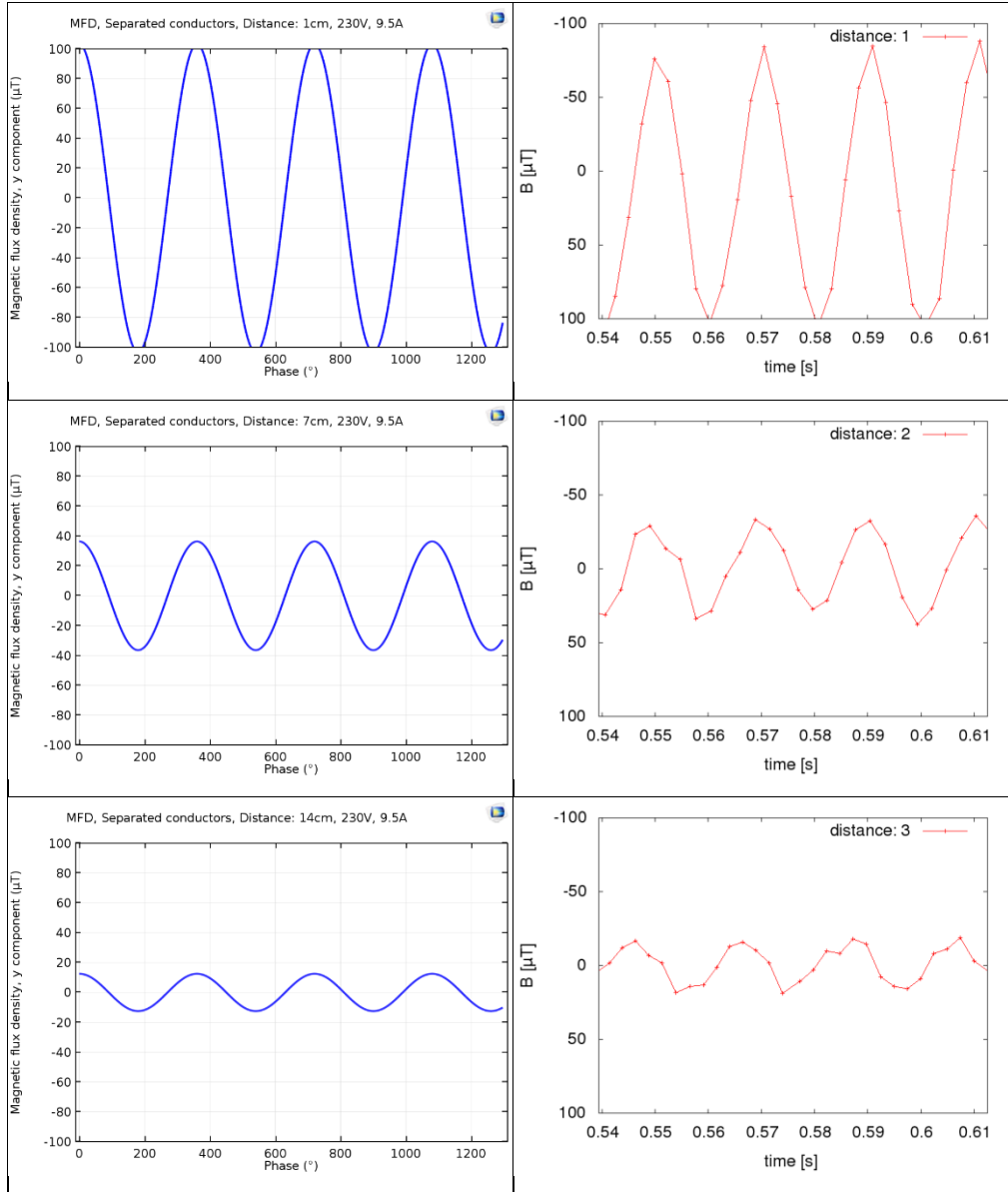Hall effect sensor of the model A1324LUA-T, which is connected to the analog-to-digital converter ADS1115. A second chosen sensor is the magnetoresistive sensor HMC1001. The ADC transmits the data via I²C-BUS to the Raspberry Pi, which saves the data and eventually monitors or processes it.
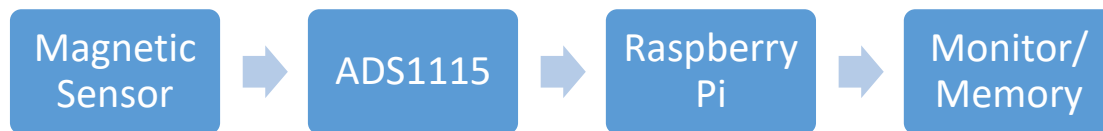
Figure 17: Block diagram of robot system

4.1 MAGNETIC FIELD SENSOR

4.1.1 Hall effect sensor

The ratiometric Hall effect sensor A1324LUA-T provides a voltage output that is proportional to the applied magnetic field. The supply voltage of 5 V fits to the Raspberry Pi. It has a relatively high sensitivity of 5 mV/G (50 mV/mT). It has a quiescent voltage output with an offset voltage of approximately 2.5 V. Therefore, this offset is mostly deleted by using the differential input of the ADC. The second input of the differential input is connected to a voltage divider.

4.1.2 AMR sensor

To decrease the noise in the signal chain the AMR sensor HMC1001 manufactured by Honeywell was used. The sensor has a higher Sensitivity of around 16 mV/G when driven with a supply voltage of 5 V. The HMC1001 consists of a Wheatstone bridge with a differential output. Therefore, a differential amplifier, in this case an instrumentational amplifier was used. After the amplifier, a filter is applied to reduce the noise. Following you can see the schematic

and the PCB layout for the analogue signal conditioning module containing the sensor, an instrumentational amplifier, a voltage converter for negative power supply, an active low pass filter and output- and supply-pinheads.
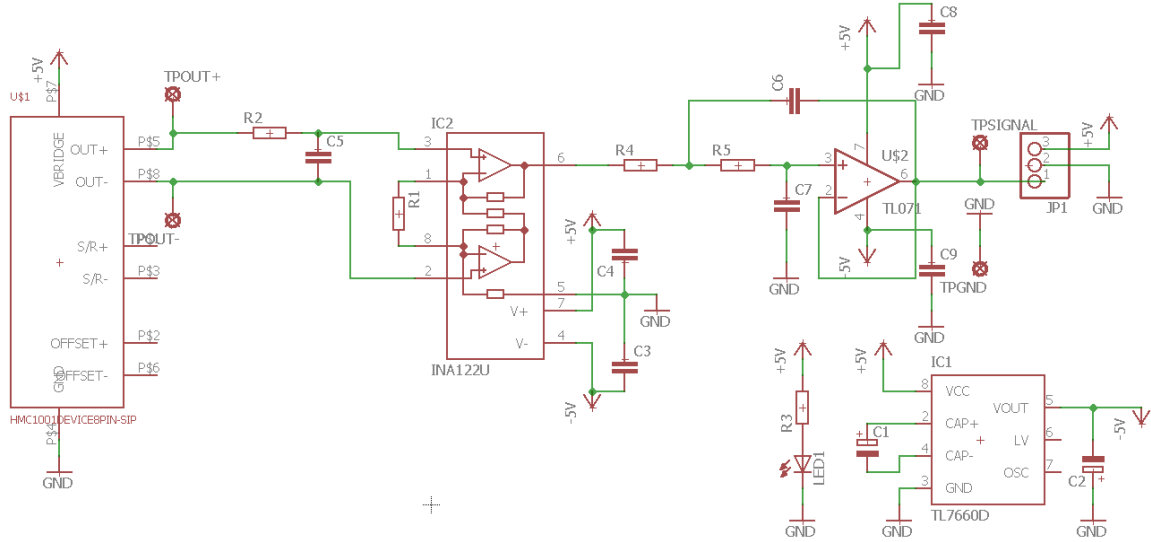

Figure 18: Schematic of Sensor Module
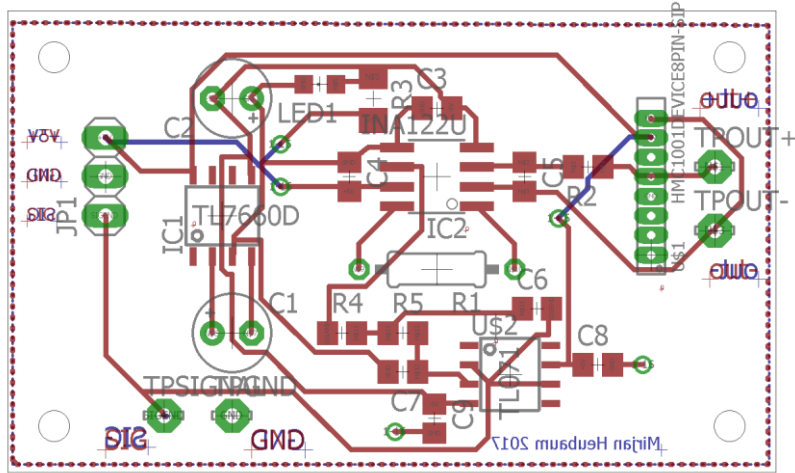
Figure 19: Layout of PCB

Figure 20 compares the noise of the Hall effect sensor and of the AMR sensor. The noise was reduced from up to 20 μTpp to lower than 1 μTpp. With this sensor, it was even possible to detect the magnetic field of a power supply cable, which carried 5 A alternating current, without separating the conductors.
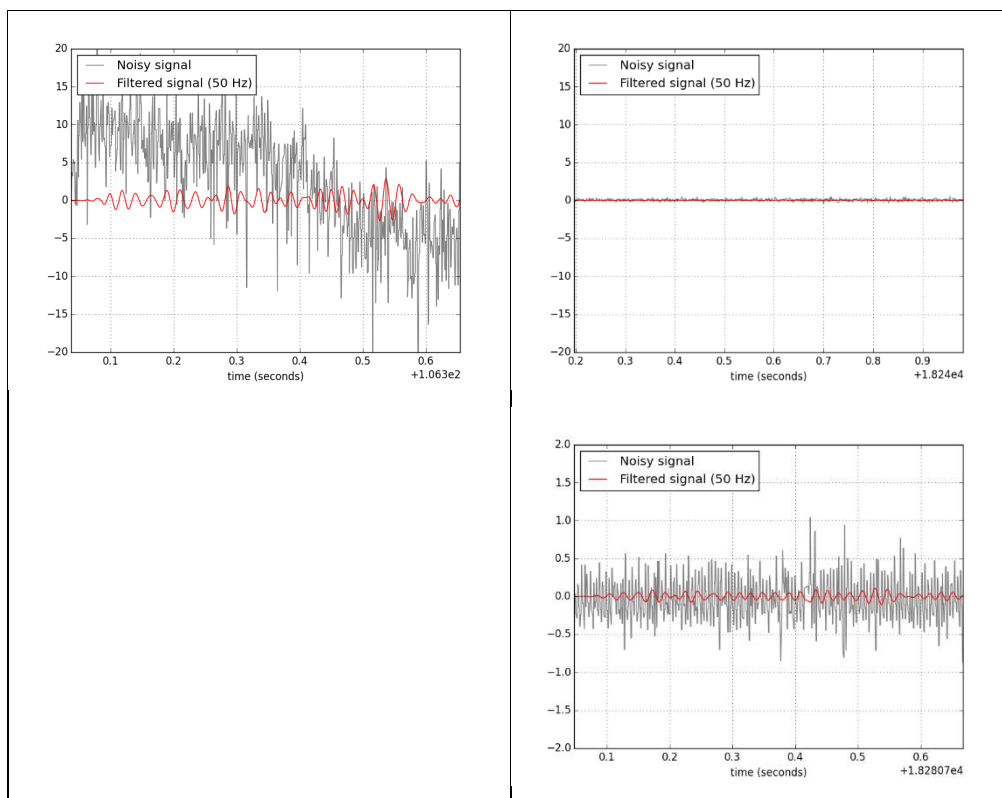
Figure 20: Noise comparison

4.1 ADC CHIP

For transmitting the data from the magnetic sensor to the Raspberry Pi an analog-to-digital
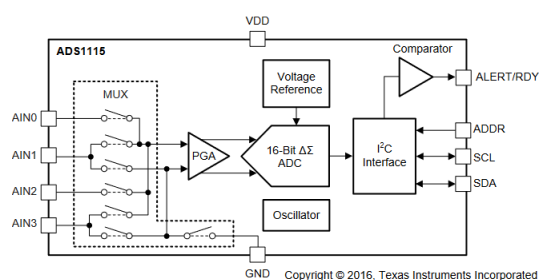
Figure 21: ADC Block Diagram

converter (ADC) is used. The chosen ADC is the ADS1115 manufactured by Texas Instruments. Regarding this purpose some features are necessary. It has four single-ended or two differential inputs AIN0 to AIN3 (cf. figure 21). In this case, both differential inputs are used. One for each

sensor. It has a programmable data rate up to 860 SPS, which is important for detecting 50 Hz signals.

The value transmitted by the ADC is a number that ranges from -32768 to 32767 because of its resolution of 16 bits. If the gain of 16 and thus a full-scale-range of ±0.256 V is chosen, the

LSB size is 7.8125 µV (cf. figure 22). That leads to 0.156 µT per LSB and a range of ±5120 µT (±51.2 G). The magnitude at the Earth's surface ranges from 25 to 65 µT and the measured signal will not be higher than 100 µT. That is why an amplifier between sensor and ADC can help to reduce the ADCs noise. With a maximum magnetic flux density of ±200µT a gain of around 20 is reasonable for a hardware based amplifier.

FSR	LSB SIZE
±6.144 V[1]	187.5 µV
±4.096 V[1]	125 µV
±2.048 V	62.5 µV
±1.024 V	31.25 µV
±0.512 V	15.625 µV
±0.256 V	7.8125 µV

Figure 22: Full-Scale Range and Corresponding LSB Size

4.2 RASPBERRY PI

The Raspberry Pi is used for computing the data and controlling the motors. Via I²C-interface the Raspberry Pi communicates with the ADC. The serial-interface is used for communication with the motor driver MD25. The user can control the Raspberry Pi itself by using WLAN and either the Secure Shell protocol (SSH) or the graphical desktop sharing system VNC. The Raspberry Pi is powered by a battery to provide its mobility.

5 Software integration and control of the robot

By using two Hall effect sensors mounted before the main body of the robot it is possible to measure where the intensity of the magnetic field is higher and therefore, to locate its origin. To solve this task three files are used on the Raspberry Pi. The two .py-files *measure.py* and *drive.py* have to be run simultaneously. The file *control.dat* serve the communication between the two running .py-programs.

- Measure.py
- Control.dat
- Drive.py

```
Read sensor left
        │
        ▼
Calculate max and min value
        │
        ▼
Read sensor right
        │
        ▼
Calculate max and min value
        │
        ▼
Left & right comparison
```

left>(right+8) → Save control value ‚l' → Speed = 3, Turn = 2

else → Save control value ‚f' → Speed = 3, Turn = 0

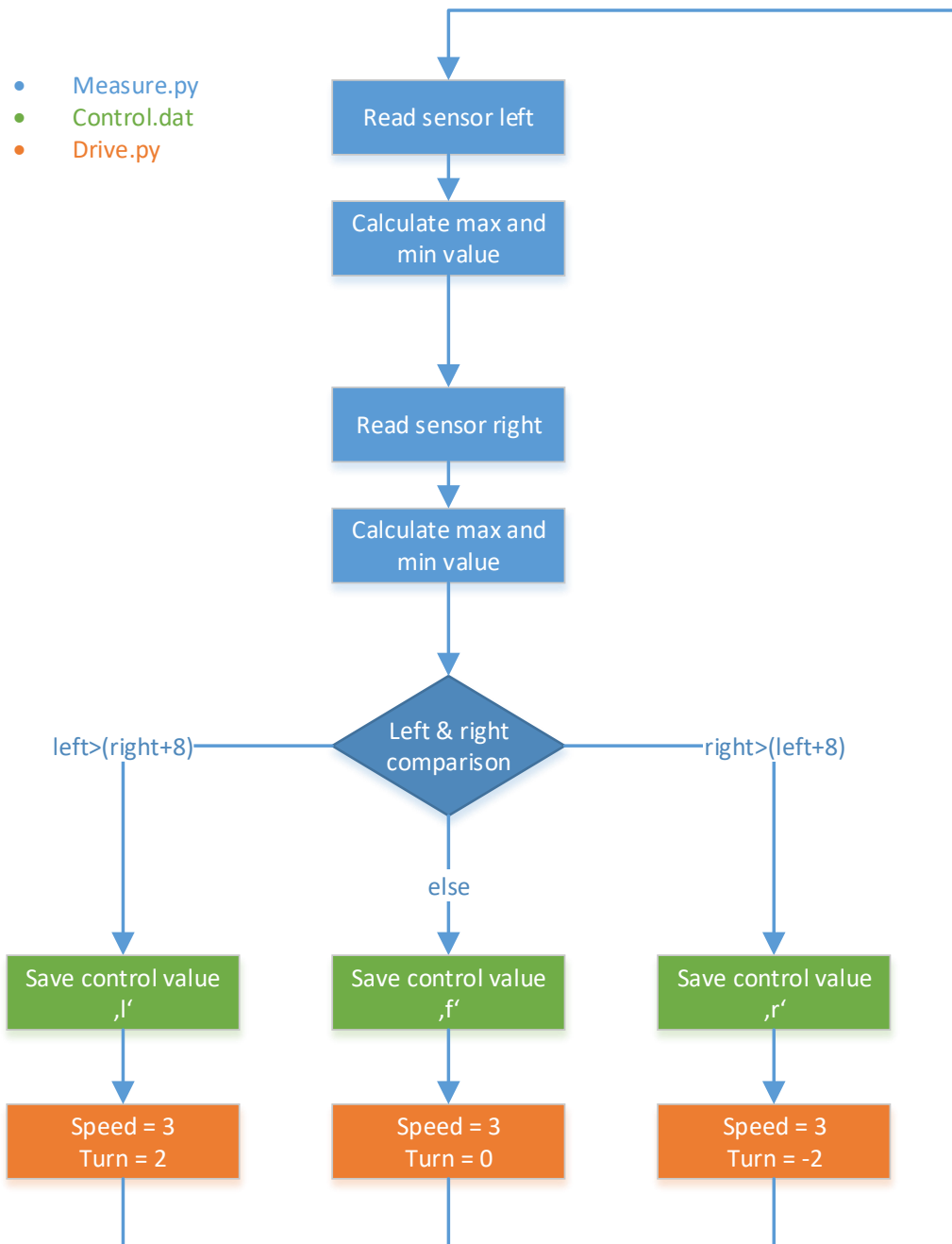right>(left+8) → Save control value ‚r' → Speed = 3, Turn = -2

Figure 23: Software structure

5.1 ALGORITHMS FOR MEASUREMENT OF MAGENTIC FIELDS

The Software has to be written in Python. The first important change in the code was to enable a higher sample rate of the ADC to be able to detect a sinusoidal wave of the magnetic field. With the sample rate of f_s=860 Hz and a supply frequency of f=50 Hz, the Nyquist–Shannon sampling theorem ($f_s > 2 * 50$ Hz) is fulfilled. That means that it is possible to measure the significant signal with the supply frequency. Then, different applications for measuring and real time plotting were programmed. The mainly used application contains of different algorithms. The first algorithm makes the mean value of a specific number of measurements. Then this value is subtracted from the following specific number of measurements. In this way, the constant component of the magnetic field is deleted. This block of measurements is now, depending on the chosen program, given to different algorithms. One counts the zero crossings of the signal and the time between them. The satisfaction of specific conditions causes a LED, mounted on the robot, to be on, when the signal looks like a sinusoidal wave. Another algorithm saves the maxima and minima of each signal (left and right), after a band-pass-filter algorithm reduced noise, and compares them. Then it decides to give the order to turn left, right or to continue straightforward. These algorithms are applied in the *measure.py* file.
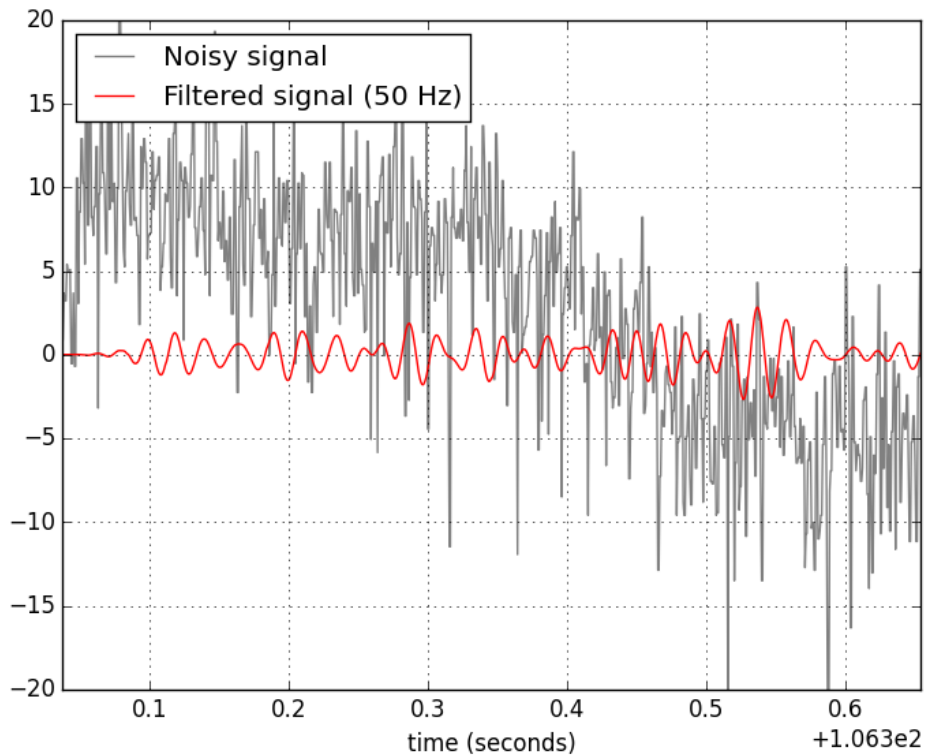
5.2 DIGITAL FILTER

Figure 24: Noisy and Filtered Signal of Hall sensor

Analog, hardware-based filters are difficult to build, if it comes to low frequencies like the supply frequency of 50 Hz. Necessary for this application is a low-pass filter, which blocks high frequencies. Even better is a band-pass filter, which also blocks lower frequencies than a predefined frequency. A band-pass filter also deletes the constant part of the signal. Therefore, a digital band-pass filter was used for this purpose. The filter is based on a python library called SciPy. As lowcut frequency 40 Hz was chosen and as high cut frequency 60 Hz was chosen. In figure 24 there is the measured, noisy signal (grey) and the filtered signal (red). The noise was reduced from up to 20 µT (peak-to-peak) to about 5 µT (peak-to-peak). The data of the filtered signal is used in the algorithms of chapter 5.1.

5.3 ALGORITHMS FOR CONTROLLING

The order to turn or to continue straightforward is saved in a file called *control.dat*. The algorithms for controlling are applied in the *drive.py* file and they make the use of the *control.dat* file. First the character saved in *control.dat* is red. Then, the variable turn is given a value depending on the character. '*f*' (forward) causes turn to be 0, '*r*' (to right) causes it to be -2 and '*l*' causes it to be 2. A predefined variable speed is set to 3. These two values are given to the function move, which sends the data and commands via the serial-interface to the MD25 motor controller.

6 Evaluation of overall function

For the final evaluation, the experimental setup from chapter 3.2 was used again. The plank with the separated conductors was mounted below a desk. Through these conductors there was again an alternating current of approximately 9.5 A. The mobile-robot started at different positions on the desk. After detecting a magnetic field with one sensor the robot turned left or right to follow the path of the cable. The photos below show the robot finding the cable and following its path.
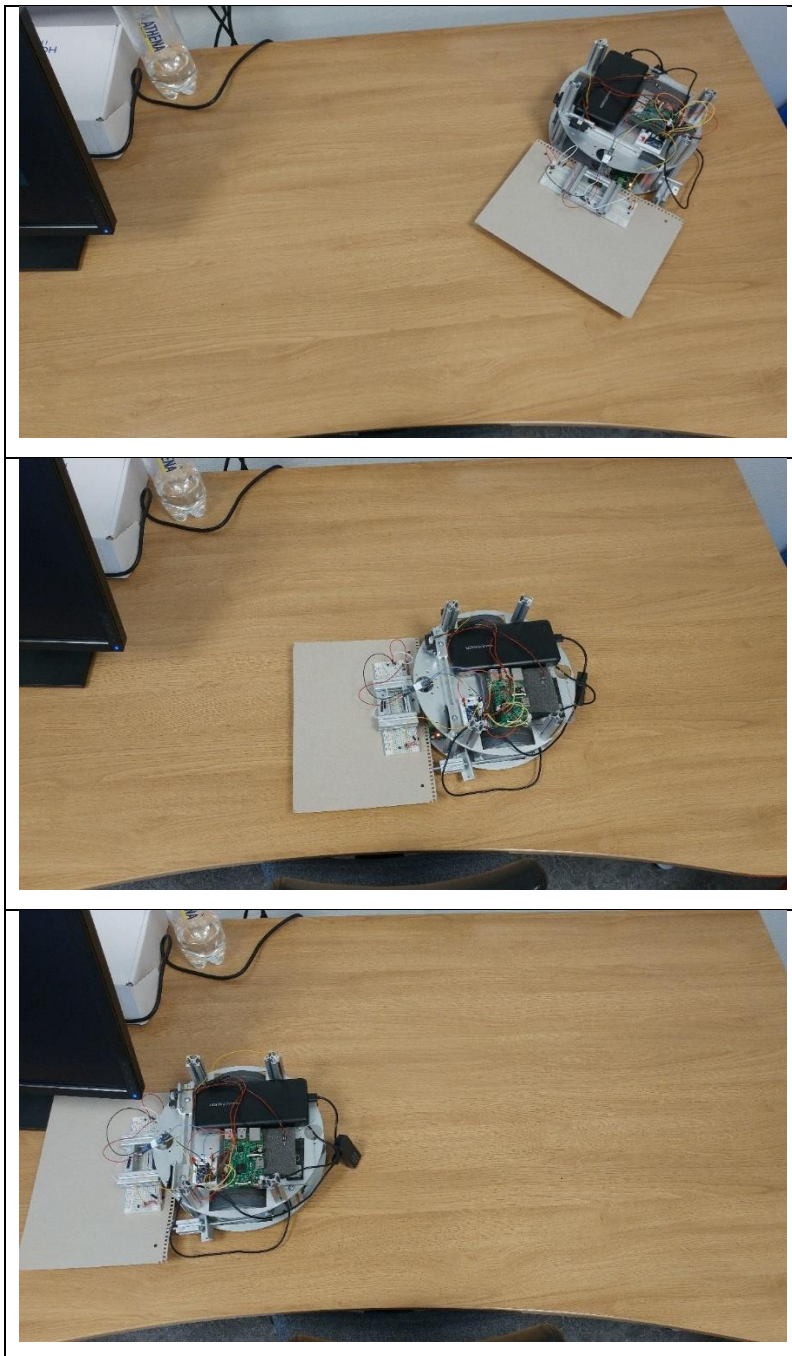
Figure 25: Cable Path Following on Desk

When positioned perpendicular to the cable, the robot started driving straight forward and during the approach of robot and cable, the magnetic flux density increased in a similar manner at the left and the right sensor. That leads the robot to go straight on and not to follow the cable path. That is why additional algorithms are needed for finding the origin of the magnetic field independent from the robots starting point.

7 Conclusion

The project fulfils its aims partially and should be continued in future works.

7.1 SUMMARY

The experimental part showed that the simulation is trustworthy because the results of the simulation and the experiment are almost equivalent. The simulation of a high-voltage three-phase underground power cable carrying 500 A current in 0.5 m depth showed that the magnetic flux density is either around 20 µT or 70 µT depending on its formation. Therefore, it might be possible to detect the magnetic field of a high-voltage underground power cable like simulated in chapter 3.1.2. Using two sensors the robot is able to follow the path of a cable with separated conductors, which carries less than 10 A under a desk. The use of the AMR sensor even made cable detection without separated conductors possible.

7.2 OUTLOOK

The next step is to detect the magnetic field of a real underground cable. The robot has to be positioned above such a cable with the aim of detecting a sinusoidal wave of the magnetic flux density. Unfortunately, the magnetic flux density of a real underground power cable depends on the current and can be very low. That is why improvements are urgently required for the systems functionality since the detection was not successful yet. The most important modification would be the construction of two PCBs containing the signal conditioning of the AMR sensor. The integration of a hardware-based low- or band-pass filter and an amplifier between sensor and ADC would reduce the noise caused by the ADC. In addition, the use of several independent sensors and the implementation of advanced cable localization algorithms would be helpful.

List of Cited Literature

[1] ETS Cable Components, "https://www.etscablecomponents.com," 06 November 2013. [Online]. Available: https://www.etscablecomponents.com/2013/11/single-core-cables-laid-trefoil-flat-formations-advantages-disadvantages/. [Accessed June 2017].

[2] P. Wang, K. F. Goddard, P. L. Lewin, S. Swingler, P. Atkins and K. Y. Foo, "Magnetic Field Measurement to Detect and Locate Underground Power Cable," American Society of Civil Engineers, 2012.

[3] C.-J. Häll and O. Torgnyson, *Detection of high-voltage power cables using electromagnetic sensing equipment on an excavator,* Gothenburg, 2015.

[4] Sun, Lee, Hou and Pong, "Underground power cable detection and inspection based on magnetic field sensing at ground surface level," 2014.

[5] Paprotny, Wright, White, Evans and Devine, "Fault Analysis in Underground Cables," University of California, 2011.

[6] J. Althaf, M. Imthiaz and R. Raj, "Underground Cable Fault Detection using Robot," International Journal of Electrical and Computer Engineering (IJECE), 2013.

[7] W. Y. Du, Resistive, Capacitive, Inductive, and Magnetic Sensor Technologies, Boca Raton: CRC Press, 2014.

[8] S. Milano, "Allegro Hall-Effect Sensor ICs," Allegro MicroSystems.

[9] J. G. Webster and H. Eren, Measurement, Instrumentation, and Sensors Handbook, CRC Press, 2014.

[10] R. Miller, "Randolph Miller's Introduction to Superconductors," [Online]. Available: http://www.wou.edu/~rmiller09/superconductivity/. [Accessed June 2017].

[11] S. Tumanski, "Induction Coil Sensors – a Review".

[12] HVPD Ltd., "An Introduction to Partial Discharge (PD)," HVPD Ltd., [Online]. Available: http://www.hvpd.co.uk/technical/. [Accessed June 2017].

List of Appendices

1. Datasheet Hall Sensor A1324
2. Datasheet AMR Sensor HMC1001
3. Datasheet ADC ADS1115
4. Datasheet Instrumentation Amplifier INA122
5. Datasheet Voltage Converter TL7660
6. Datasheet Op. Amp. TL071